Relationships between the winding angle, the characteristic radius, and the torque for a long polymer chain wound around a cylinder: Implications for RNA winding around DNA during transcription

Boris P. Belotserkovskii*

Department of Biology, Stanford University, 371 Serra Mall, Herrin Labs, Stanford, California 94305-5020, USA

(Received 22 November 2013; published 10 February 2014)

Long polymer chains are ubiquitous in biological systems and their mechanical properties have significant impact upon biological processes. Of particular interest is the situation in which polymer chains are wound around each other or around other objects. We have analyzed the parameters of a long Gaussian polymer chain wound around a cylinder as a function of the torque applied to the ends of the chain. We have shown that for sufficiently long polymer chains, an average winding angle and a characteristic radius of the chain can be determined from a modified Bessel function of purely imaginary order, in which the value of the order is equivalent to the applied torque, normalized to the product of the absolute temperature and the Boltzmann constant. The obtained results are consistent with a simplified interpretation in terms of "torsional blobs," and this could be extended to nonideal chains with excluded volumes. We have also extended our results to the case of a polymer chain rotating in viscous medium. Our results could be used to estimate the mechanical strains that appear in DNA and RNA during transcription, as these might initiate formation of unusual DNA structures, invasion of RNA into the DNA duplex (*R*-loop formation), and modulation of the interactions of DNA and RNA with proteins.

DOI: 10.1103/PhysRevE.89.022709 PACS number(s): 87.14.G−, 82.35.Lr, 87.15.−v

I. INTRODUCTION

The winding of random walk trajectories around a given domain in space, for example, an impenetrable obstacle, has received significant attention and has multiple implications for polymer physics ([1,2], and references therein). In general, the winding of a polymer chain around an obstacle decreases the chain entropy and consequently creates forces directed to unwinding; if the unwinding is impossible (for example, due to anchoring of the chain's ends), these forces would create mechanical strains and deformations within the system. We have suggested that this effect might appear during DNA transcription, if the nascent RNA becomes anchored to the DNA [Fig. 1(a)] [3]. In this case, because RNA polymerase rotates relative to DNA during transcription, the nascent RNA becomes wound around DNA. Winding-induced mechanical strain within the nascent RNA exerts a torque upon the double-stranded DNA region over which the nascent RNA is wound, which would cause negative supercoiling in this DNA region; that, in turn, could cause a number of biologically important phenomena such as unusual DNA structure formation, RNA invasion into the DNA (*R*-loop formation), modulation of protein binding, etc. This strain would also be expected to destabilize the transcription complex, thereby increasing the probability of transcription termination. Importantly, the anchoring-induced "static" supercoiling depends only upon the number of turns (per RNA length), which the nascent RNA has made around the DNA between the anchoring point and the RNA polymerase; in contrast to "dynamic" transcription-driven supercoiling (see below), anchoring-induced supercoiling does not depend upon the viscosity of the medium, or upon the absolute rotational rates of RNA polymerase and DNA during transcription. Thus, it does not matter whether the RNA polymerase is actually revolving around the DNA, or whether it is fixed while the DNA is rotating, as suggested in the "transcription factory" model [4].

In previous calculations we primarily considered the situation of "tight wrapping," in which the anchoring occurs close (in terms of length of the nascent RNA) to the transcribing RNA polymerase. In that case the estimated torque appeared to be so large that it would cause either disruption of the anchoring and/or the transcription complex, or, more likely, the nascent RNA invasion into the double-stranded DNA (i.e., *R*-loop formation) [3].

In the present work, we consider the more general case that includes a "loose" wrapping of the polymer chain around an obstacle. In the case of transcription, this situation could appear when anchoring has occurred at a later time after the start of transcription, when a sufficiently long transcript has already been produced. A very large size and slow synthesis of certain transcripts (e.g., [5]) could facilitate this scenario.

Upon continuation of transcription, the relative contribution from the initial RNA "slack" to RNA winding around DNA decreases, the winding becomes tighter, and the winding-induced negative supercoiling increases (in the limit approaching a very high value for the tight wrapping without initial slack, estimated in [3]), and eventually this negative supercoiling would be large enough to trigger *R*-loop formation.

R loops have a number of important biological functions (e.g., [6–9]), but they are also a source of genomic instabilities (e.g., [10,11]) and they are implicated in partial transcription blockage by certain nucleotide sequences [12–14], which makes them possible substrates for a "gratuitous" form of transcription-coupled DNA repair ([15], reviewed in [16]). The probability of *R*-loop formation by a given sequence is usually defined by the stability of the RNA-DNA hybrids formed by this sequence [17]. However, the nascent RNA anchoring by the mechanism shown in Fig. 1(a) would facilitate *R*-loop formation in any transcribed sequence regardless of the stability of RNA-DNA hybrids formed by this sequence.

*borisbp@stanford.edu

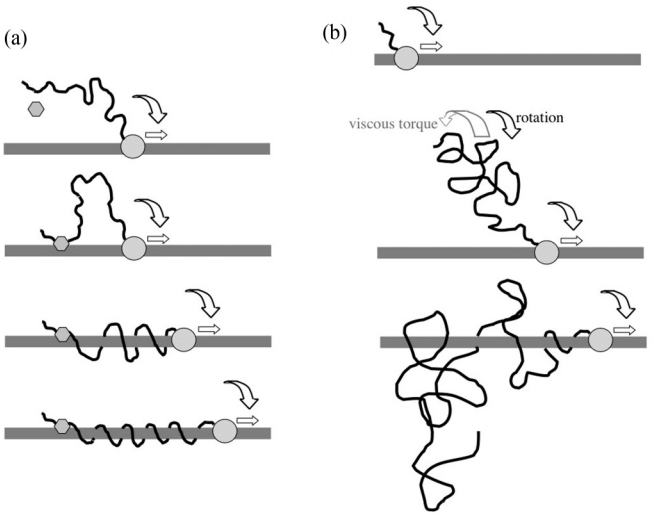

FIG. 1. Cotranscriptional nascent RNA winding around DNA. (a) Nascent RNA winding around DNA caused by RNA anchoring. RNA polymerase (gray oval) is transcribing DNA (shown by a thick gray line) producing a nascent transcript (shown by a thinner black line). White block arrows with black borders show directions of translational movement and rotation of RNA polymerase relative to DNA during transcription. Next, nascent RNA becomes anchored to DNA by some anchoring agent (for example, bivalent RNA-DNA binding protein) shown by a gray hexagon. Because RNA polymerase rotates relative to DNA, further transcription would cause RNA wrapping around DNA, which is tightening upon continuation of transcription. This tightening wrapping would produce growing negative supercoiling in the wrapped region of DNA [3], which would eventually cause RNA invasion into the DNA duplex producing an *R* loop (not shown). In the case of a sufficiently long wrapped DNA region wrapping-induced supercoiling could produce plectonemic supercoils in this region (not shown). (b) Nascent RNA winding around DNA caused by viscous resistance against nascent RNA rotation during transcription. Rotation of RNA polymerase relative to DNA causes nascent RNA to rotate in the same direction. Viscous resistance against this rotation creates a torque acting in a direction opposite to rotation (shown by block arrow with gray borders), which tends to wind nascent RNA around DNA. Because RNA winding around DNA is energetically unfavorable due to decrease in RNA entropy upon winding, RNA resists winding, and consequently, winding would become pronounced only when the transcript would reach sufficiently large length to create viscous torque sufficient to counteract spontaneous entropy-driven RNA unwinding. Because a given region of the RNA chain experiences viscous torque created by all RNA regions localized between this region and the free end of the nascent RNA, the farther this region is from the free end (i.e., the closer it is to RNA polymerase), the larger the torque, and, consequently, the tighter the RNA winding. Note that for easier visualization of RNA regions with different degrees of winding, linear stretching of the nascent RNA along the direction of transcription is strongly exaggerated (see Sec. II C).

The anchoring could be performed by a "bivalent" protein, which is capable of binding RNA and DNA simultaneously. An important example of such a protein is transcription factor YY1, for which simultaneous cotranscriptional binding to nascent RNA and to DNA has been implicated in the regulation of gene silencing [18,19]. Similar modes of protein-mediated cotranscriptional nascent RNA binding to DNA have been suggested for the regulation of the dihydrofolate reductase gene [20] and for the Z-DNA binding protein (which at the same time is an RNA-editing enzyme so it should be able to bind RNA, at least transiently) (review in [21,22]). In general, there is a growing number of examples of protein-mediated RNA-DNA binding (e.g., reviewed in [19]); thus, one could expect that cotranscriptional nascent RNA anchoring might also be common in living cells. Other forms of RNA-DNA interactions, including triplex formation [23,24], could also produce this type of anchoring. Some unusual DNA structures, such as H-DNA (reviewed in [25,26]), contain single-stranded regions which could readily hybridize with the nascent transcript provided that they have sufficient homology. Yet another example of this type of anchoring is the "hybrid" quadruplex between RNA and DNA, which has been implicated in *R*-loop-mediated replication initiation in mitochondria [27].

Another important phenomenon in which the effect of nascent RNA winding around DNA could have a significant contribution is dynamic transcription-induced supercoiling caused by viscous resistance against the relative rotation of transcription machinery (together with nascent RNA) and DNA ([28], reviewed in [29]). In this case, although the distal end of the nascent RNA is not anchored to DNA, the torque induced by viscous resistant forces could be sufficient to cause nascent RNA winding around DNA [Fig. 1(b)]; this would decrease the effective gyration radius of the RNA, thus decreasing its apparent friction coefficient, and consequently decreasing the torque. This "negative feedback" due to RNA winding should be taken into account when estimating the transcription-induced supercoiling. However, in the absence of anchoring, a sufficiently large viscous resistance for nascent RNA motion is essential for RNA winding, because the mechanical strains in the wound RNA would facilitate its spontaneous unwinding via random thermal motions, and if the viscous resistance to those motions were small, the unwinding would occur very rapidly without accumulated winding. Thus, in the absence of anchoring, the nascent RNA winding would become pronounced only after some sufficiently large length of transcript had been generated; the estimation of this "critical" length would be important for evaluation of the mechanical strains that appear in DNA and RNA during transcription.

The interdependence between torque, winding, and characteristic size for the polymer chain is of significant importance. We have rigorously analyzed these dependences for the model of a very long ideal Gaussian polymer chain, and have also made approximate estimations for nonideal chains with excluded volume and for chains rotating in viscous media.

II. RESULTS AND DISCUSSION

A. Ideal Gaussian chain wound around a cylinder

Under a constant torque, a very long ideal Gaussian chain wound around a cylinder is described by a modified Bessel equation of purely imaginary order, where the absolute value of the order is equivalent to the torque normalized upon the thermal energy kT.

In the continuous approximation, the statistical weight *W* of the Gaussian chain comprising *N* segments is described by

the diffusionlike equation ([2] and references therein),

$$\frac{\partial W}{\partial N} = \frac{l^2}{2}\nabla^2 W. \tag{1}$$

Here l is the length of the chain segments divided by the square root from the system dimensionality (e.g., by $\sqrt{3}$ in the case of three dimensions).

In general, we are interested in simultaneous chain winding around a cylinder and the chain stretching along the cylindrical axis, but because the Gaussian chain deformations in different directions are independent, we can consider these two deformations separately. To analyze the chain wrapping around a cylinder, we consider a two-dimensional version of Eq. (1) in the polar coordinates:

$$\frac{\partial W}{\partial N} = \frac{l^2}{2}\left(\frac{\partial^2 W}{\partial r^2} + \frac{1}{r}\frac{\partial W}{\partial r} + \frac{1}{r^2}\frac{\partial^2 W}{\partial \phi^2}\right), \tag{2}$$

where r is the distance from the cylinder axis, and ϕ is the winding angle around this axis. If a constant torque M is applied to the chain, then the average winding angle would be

$$\langle\phi\rangle = \frac{\int_{-\infty}^{+\infty}\phi W\exp\left(\frac{M\phi}{kT}\right)d\phi}{\int_{-\infty}^{+\infty} W\exp\left(\frac{M\phi}{kT}\right)d\phi} = \frac{\partial\left(\ln W_M\right)}{\partial\left(\frac{M}{kT}\right)}, \tag{3}$$

where

$$W_M = \int_{-\infty}^{+\infty} W\exp\left(\frac{M\phi}{kT}\right)d\phi = \int_{-\infty}^{+\infty}\exp\left(\frac{kT\ln W + M\phi}{kT}\right)d\phi. \tag{4}$$

Note that the convergence of this integral for $\varphi \to \infty$ is ensured by a finite value of the cylinder radius, because for sufficiently tight winding around a cylinder, the energy of the chain deformation becomes quadratic upon ϕ, thus growing faster than the torque-dependent term $M\phi$.

Multiplying Eq. (2) by $\exp(\frac{M\varphi}{kT})$ and integrating over $-\infty < \varphi < +\infty$, we obtain

$$\frac{\partial W_M}{\partial N} = \frac{l^2}{2}\left(\frac{\partial^2 W_M}{\partial r^2} + \frac{1}{r}\frac{\partial W_M}{\partial r} + \frac{\left(\frac{M}{kT}\right)^2}{r^2}W_M\right). \tag{5}$$

We are interested in the solution for very long chains, for which the distribution of the segments' positions relative to the cylinder as well as an average winding per segment does not depend upon the length of the chain and upon initial conditions, but depends only upon torque.

We will look for such a solution in the form

$$W_M(N,r) = g(r)\exp\left(\frac{a^2 N}{2}\right), \tag{6}$$

where $g(r)$ is some finite function. Equation (6) cannot account for the condition in which the end segments of the chain are attached to the surface of the cylinder; rather, their distance from the cylinder axis would be distributed as $g(r)$, as for all other segments. However, for sufficiently long chains the precise manner of attachment should not affect the results.

It is also important to note that although our derivations below are performed for the chain under a fixed torque, for sufficiently long chains the torque-winding dependence would be the same as for the chain with a fixed winding density, which is defined by the equation

$$M = -\frac{\partial kT\ln W}{\partial\phi}. \tag{7}$$

This equation corresponds to the condition in which the function under the integral in Eq. (4) reaches a maximum. The sharpness of this maximum would grow with increasing N, and thus the value of ϕ, at which the under-integral function reaches the maximum, would provide the predominant contribution to the average value of ϕ.

Substituting Eq. (6) into Eq. (5), and designating

$$x \equiv r\frac{a}{l}, \tag{8}$$

$$q \equiv \frac{M}{kT}, \tag{9}$$

we obtain

$$x^2\frac{d^2 g}{dx^2} + x\frac{dg}{dx} + (q^2 - x^2)g = 0. \tag{10}$$

This is a modified Bessel equation of purely imaginary order iq.

Characteristic parameters of the chain can be obtained from the dependence of the largest zero of the modified Bessel function of the second kind of purely imaginary order, upon the absolute value of the order.

In our case, the solution of Eq. (10) must reach zero at the surface of the cylinder (i.e., for $r = R$), be positive for $r > R$, and approach zero when r approaches infinity rapidly enough that the integral $\int_R^\infty g(r)rdr$ is finite.

The solution that satisfies these requirements is the modified Bessel function of the second kind (also known as the modified Hankel function, the modified Bessel function of the third kind, and some other designations) of purely imaginary order $K_{iq}(x)$ ([30], and references therein).

In the interval between $x = 0$ and a certain positive value $x = x_1(q)$ (further referred to as the largest zero of the function), this function is oscillating between negative and positive values an infinite number of times until it switches from negative to positive value for the last time at $x = x_1(q)$, and then remains positive, first reaching a local maximum, and then monotonically decreasing, approximately as $\frac{e^{-x}}{x^{1/2}}$.

Because $g(r)$ is positive, and must be zero at the surface of the cylinder ($r = R$), the largest zero of the function should correspond to the surface of the cylinder. Thus, from Eq. (8) we obtain

$$x_1 = R\frac{a}{l}. \tag{11}$$

The dependence $x_1(q)$ (for which the general analytical expression is unknown, but numerical estimations and asymptotics are available; see below), defines all physical parameters for a sufficiently long Gaussian chain to which a torque $M = kTq$ is applied.

From Eq. (6), the free energy of the chain is

$$-kT\ln W_M \approx -kT\frac{a^2 N}{2} = -NkT\frac{l^2}{R^2}\frac{x_1^2}{2}. \tag{12}$$

From Eqs. (3) and (12), the average winding per segment (referred to further as the average winding density) is

$$u \equiv \frac{\langle\phi\rangle}{N} = \frac{\partial\left(\ln W_M\right)}{\partial\left(\frac{M}{kT}\right)}\frac{1}{N} \equiv \frac{\partial\left(\ln W_M\right)}{\partial q}\frac{1}{N} \approx \frac{1}{2}\left(\frac{l}{R}\right)^2\frac{d\left\langle x_1^2\right\rangle}{dq}. \tag{13}$$

The above equation provides a general expression for winding-torque dependence [$u = u(q)$, or $q = q(u)$] for a sufficiently long Gaussian chain wound around a cylinder. (Below, unless otherwise indicated, we will consider only sufficiently long chains, for which the results obtained for infinitely long chains are good approximations, and use "=" instead of "≈" if we imply the limit for $N \to$ infinity).

Characteristic distance scale of the chain could be interpreted as a "torsional blob" size. From Eqs. (8) and (11) it follows that the value

$$r_b = \frac{l}{a} = \frac{R}{x_1} \tag{14}$$

defines some characteristic distance scale for the infinitely long chain under a given torque. Substituting Eq. (14) into Eq. (12) for free energy, we obtain

$$-kT\ln W_M \approx -\frac{kT}{2}\frac{Nl^2}{r_b^2} \sim -kT\frac{r_N^2}{r_b^2}, \tag{15}$$

where r_N is the size of an unperturbed random coil containing N segments. From Eq. (15) it is seen that when the size of the unperturbed coil is equivalent to r_b, the free energy of the coil under applied torque is about kT (i.e., the energy of random thermal fluctuation). From that, we could interpret r_b as the size of the coil at which perturbations caused by forces applied to the coil are of the same magnitude as random thermal fluctuations of the coil. For the coils of sizes below this size, perturbations caused by applied forces could be neglected, while for the coils of sizes above this size, the effect of applied forces upon the coil deformation is stronger than the effect of thermal fluctuations. A coil of this threshold size is referred to as a blob (reviewed in [31]). Sometimes we will refer to it as a torsional blob, by analogy with "tensile blob" defined by the linear stretching force [32]. We will discuss a simplified blob-based analysis as applied to polymer chain winding in more detail in Secs. II B and II C, in which we consider nonideal chains and chains rotating in viscous medium.

Analysis based upon asymptotic expressions for the largest zero of the modified Bessel function of the second kind of purely imaginary order for small and for large orders, shows that at small torques the torque-winding dependence is nonlinear, and the characteristic distance scale is much larger than the radius of the cylinder; while at large torques, torque-winding dependence is linear, and the characteristic distance scale is much smaller than the radius of the cylinder.

As already mentioned, the general analytic expression for $x_1(q)$ is unknown. However, asymptotic expressions have been obtained for large and small values of q [30]:

For $q < 1$ (i.e., small torque $M < kT$), from Eq. (8) from the above cited manuscript,

$$x_1(q) \approx C\exp\left(-\frac{\pi}{q}\right), \tag{16}$$

where the numerical constant $C = 2\exp(-\gamma) = 1.1\cdots$ ($\gamma = 0.57\cdots$ is the Euler-Mascheroni constant) is close to 1 and can be omitted in further analysis.

Substituting Eq. (16) into Eq. (13), we obtain the winding-torque interdependence for small torques:

$$u \approx \pi\left(\frac{l}{R}\right)^2\frac{1}{q^2}\exp\left(-\frac{2\pi}{q}\right), \tag{17}$$

or taking the logarithm of this equation, and taking into account that for $q < 1$, $1/q > \ln(1/q)$,

$$M \approx \frac{2\pi kT}{\ln\frac{1}{u}}. \tag{18}$$

This dependence is nonlinear, because in this regime the characteristic distance from the axis of the cylinder, which defines the lever arm for deformational forces, strongly depends upon the chain winding (see below).

Substituting Eq. (16) into Eq. (14), we obtain the size of the blob for small torques:

$$r_b \approx R\exp\left(\frac{\pi}{q}\right). \tag{19}$$

Because for $q < 1$ this value is significantly larger than the radius of the cylinder, it can be considered as the only characteristic scale describing the distance from the chain to the cylinder, and it could be used as an estimate for both distance from the surface of the cylinder and from its axis. Combining Eqs. (17) and (19), we obtain

$$u \approx \frac{\left(\ln\frac{r_b}{R}\right)^2}{\pi}\frac{l^2}{r_b^2}, \tag{20}$$

or, up to smaller logarithmic terms,

$$\ln\frac{1}{u} \sim \ln\frac{r_b^2}{l^2}. \tag{21}$$

For the large torque approximation $M/kT \equiv q > 1$, Eq. (16) is replaced by

$$x_1(q) \approx q \tag{22}$$

(Eq. (18) in [30]).

Substituting Eq. (22) into Eq. (13) we obtain "Hooke's" direct proportionality between the torque and the average winding density:

$$u \approx \left(\frac{l}{R}\right)^2 q = \left(\frac{l}{R}\right)^2\frac{M}{kT}. \tag{23}$$

For the blob size for large torques we obtain

$$r_b \approx \frac{R}{q} = \frac{R}{\left(\frac{M}{kT}\right)} \approx \frac{l^2}{Ru}. \tag{24}$$

As expected, for finite R, upon $M \to \infty$, $r_b \to 0$, which is consistent with the chain becoming tightly wound around the cylinder. Note, however, that for the tight winding, the blob size is not equivalent to the characteristic distance h_c from the chain to the surface of the cylinder, which also approaches zero at finite R and $M \to \infty$, but scales differently than r_b

with these parameters:

$$h_c \sim \frac{R}{\left(\frac{M}{kT}\right)^{2/3}} \sim \frac{l^{4/3}}{u^{2/3} R^{1/3}} \tag{25}$$

(for derivation, see Appendix A).

Because at large torque, the distance from the surface h_c is significantly smaller than the radius of the cylinder, the stretching of the segment in the direction of the winding $l\uparrow = u(R + h_c) \approx u\,R$, and the stretching force $F = M/(R + h_c) \approx M/R$. Consequently, at large torques Eq. (23) approaches the well-known expression for the relative extension of the ideal Gaussian chain in the direction of the force: $l\uparrow/l = (F\,l)/kT$, and Eq. (24) approaches the expression for the tensile blob size for one-dimensional force F: $r_b = kT/F$ [32].

Using the torque-winding dependence obtained in this section, we can estimate the amount of supercoiling induced by the nascent RNA winding around DNA (see Appendix B).

B. Simplified analysis of the nonideal chains with excluded volume

For the simplified analysis of nonideal chains, we will use a notion of a blob, which is the coil where the characteristic sizes of directed distortions created by some external force are of the same magnitude as the random distortions produced by thermal fluctuations in the absence of an external force. Consequently, all average geometric parameters of the blob-size coil are of the same magnitude, as that for the coil with the same number of segments in the absence of external forces. For example, for one blob, the relationship between the characteristic size r_b and the number of the segments N_b, is roughly the same as for an unperturbed coil:

$$r_b \sim l N_b^{\nu}, \tag{26}$$

where ν is the Flory exponent (here and below we assume for simplicity that the segment of the chain has only one characteristic size l, and this size is about the same as the radius of the cylinder R).

For the blob-size coil, distortions induced by external forces are of the same magnitude as the respective geometrical parameters of an unperturbed coil with the same number of segments. Thus, for one blob, the value of the average winding angle $\langle\phi\rangle$ generated by the torque is roughly the same as the characteristic absolute value ϕ_0 of the winding angle for the random winding of a coil containing the same number of segments in the absence of torque. Thus,

$$u \equiv \frac{\langle\phi\,(N_b)\rangle}{N_b} \sim \frac{\phi_0\,(N_b)}{N_b}. \tag{27}$$

From the analogy with tensile blobs (where torque is an analog of force, and winding angle is an analog of the linear coordinate),

$$\frac{1}{q} \equiv \frac{kT}{M} \sim \langle\phi\,(N_b)\rangle \sim \phi_0\,(N_b)\,. \tag{28}$$

For sufficiently large N_b (which in our case means large blob size, or small torque),

$$\phi_0\,(N_b) \sim (\ln N_b)^{\kappa}\,, \tag{29}$$

where the parameter κ for an ideal Gaussian chain $= 1$ (reviewed in [2]). For two-dimensional chains with excluded volume $\kappa = 0.5$ (reviewed in [33]); for three-dimensional chains with excluded volume, the analytically predicted value is also 0.5 [34], but computer modeling produced $\kappa = 0.75$ [35].

Combining Eqs. (26)–(29), we obtain

$$\ln N_b \sim \frac{1}{q^{1/\kappa}}, \tag{30}$$

$$\ln\frac{1}{u} \approx \ln N_b - \ln(\ln N_b)^{\kappa} \sim \frac{1}{q^{1/\kappa}} + \ln q \approx \frac{1}{q^{1/\kappa}}, \tag{31}$$

$$\ln\frac{r_b}{l} \approx \ln N_b^{\nu} \sim \frac{\nu}{q^{1/\kappa}}, \tag{32}$$

$$\ln\frac{1}{u} \approx \ln\left(\frac{r_b}{l}\right)^{1/\nu}. \tag{33}$$

(Here "$\sim$" implies "up to numerical coefficients about unity," and "$\approx$" means "up to smaller terms"). For an ideal Gaussian chain, for which $\nu = 0.5$, $\kappa = 1$, the results of Eqs. (31)–(33) coincide with approximations for results obtained from more rigorous model analysis [Eqs. (18), (19), and (21), respectively].

In the large torque limit, the wound chain could be approximated by a one-dimensionally stretched chain (see comments below Eq. (25) in previous subsection), for which force-extension dependences for various polymer chain models are available; thus we are not analyzing that case in this subsection.

C. Analysis of the rotating polymer chain in viscous medium

In the this subsection, we will extend our analysis to the polymer chain for which one end is free, while the other end is attached to the surface of the cylinder, and can rotate relative to the axis of the cylinder while remaining attached to the surface. As mentioned in the Introduction, this could model the behavior of the nascent RNA chain during transcription [Fig. 1(b)].

In the steady state, the entire chain would rotate with the same angular velocity as the attached end. During rotation the chain would experience a torque generated by viscous friction, which would tend to wind the chain around the cylinder. The closer the region of the chain to the attachment point, the larger the local torque applied to the ends of this region, and, consequently, the tighter would be its wrapping around the cylinder; i.e., the characteristic distance between the chain and the cylinder decreases from the free end to the attachment point. A similar situation appears when the polymer is dragged by the end in viscous medium, where it forms either a "trumpet" or "stem-flower" profile [36–39].

We are going to evaluate the profiles of the characteristic distance and the torque as a function of the distance along the chain for the rotating polymer chain, using the results developed in the previous section.

Similar to the analysis of the chain dragged by a force in viscous medium, we will use the notion of the blob size $r_b = r_b(M)$, which is the characteristic size below which deformation of the coil by torque M can be neglected. The

larger the torque, the smaller the size of the blob. (Note that, rigorously speaking, the relationship $r_b(M)$, which we are going to use in this analysis, is derived for the torque applied to the ends of the chain, while in the case of a rotating chain, viscous forces are acting upon each segment of the chain. However, in our simplified analysis, we assume that for each blob the entire viscous resistance of the blob is concentrated at the end of the blob proximal to the free end of the chain; thus, the torque is applied to the ends of the chain region within one blob. Alternatively, one can proceed directly to the continuous model, similar to that described in [36–39].)

Let us consider the behavior of a rotating chain as a function of its length. When the chain is very short, its respective coil size, and consequently its viscous resistance, is small; thus, the viscous torque generated by its rotation is also small, and the respective blob size which corresponds to this small torque is large; thus for the small length, the size of the unperturbed coil which corresponds to this length is smaller than the size of the blob, and consequently the chain shape is practically unperturbed by rotation (i.e., nonrandom winding of the chain around a cylinder is not pronounced). Upon increasing the chain length, the size of the coil also increases, leading to an increase in torque and a decrease of the respective blob size. At some critical length, the size of the unperturbed coil becomes equal to the size of the blob (which we will call the "first blob"). Starting from this critical first blob length, nonrandom winding of the chain around the cylinder becomes noticeable. If the chain is longer than the critical length, it forms a second blob, for which the size is defined by the sum of viscous torques created by the first blob and by the second blob itself, and so forth. In general, if M_j is the torque acting upon a blob with the number j, μ_j is the viscous rotational resistance of this blob, and ω is the angular rate of rotation. Then

$$M_j = \sum_{i=1}^{i=j} \omega \mu_i. \tag{34}$$

In particular, for the very first blob,

$$M_1 = \omega \mu_1. \tag{35}$$

Let N_{bj} be the number of segments in the blob number j. Then, the distance (expressed in the number of segments) from the blob number j to the free end of the chain is

$$s_j = \sum_{i=1}^{i=j} N_{bi}. \tag{36}$$

From these two equations, an "artificial" variable j can be excluded, and the torque could be expressed as a function of the distance from the free end. In the continuous approximation, that leads to the equation

$$\frac{dM}{ds} = \omega \frac{\mu}{N_b}. \tag{37}$$

Recurrent calculations using Eq. (34) or its continuous analog Eq. (37) can be continued until the distance from the end [Eq. (36)] becomes equivalent to the total length of the chain, or until the torque become so large that the size of the blob becomes smaller than the size of the segment (as in the stem-flower profile [38]); consequently, the blob-based analysis would become nonapplicable and should be replaced by some other model applicable to strongly stretched chains. Note that for continuous Eq. (37), the condition at the free end $M(s=0)=0$ implies that $r_b(s=0)=\infty$. This divergency, which was previously discussed for the trumpet model [39], could be circumvented by starting calculation from the first blob, i.e., from $s = N_{b1}$.

In the absence of hydrodynamic interactions between the segments within a blob,

$$\mu \sim N_b l \eta \langle r^2 \rangle, \tag{38}$$

where $\langle r^2 \rangle = \langle r^2 \rangle (r_b, R)$ is the average quadratic distance of the segment from the cylindrical axis, $\langle r^2 \rangle \sim r_b^2$ at small torques, and $\langle r^2 \rangle \approx R^2$ at large torques.

Equations (37) and (38) allow us to evaluate the profiles of the characteristic distance and the torque as a function of the distance along the chain for the rotating polymer chain, in the absence of hydrodynamic interactions. However, because the general analytic expression for function $r_b(M)$ is unknown, we cannot write the general analytic solution for this equation for all values of torques.

Here we will limit an analysis to the small torques, for which $r_b > R$; thus $\langle r^2 \rangle^{1/2} \sim r_b$, and from Eq. (19),

$$\frac{M}{kT} \approx \frac{\pi}{\ln (r_b/R)}. \tag{39}$$

Introducing the dimensionless blob size,

$$\chi \equiv \frac{r_b}{R}, \tag{40}$$

and substituting Eqs. (38)–(40) into Eq. (37), we obtain

$$-\frac{1}{(\ln \chi)^2 \chi^3} \frac{d\chi}{ds} = \frac{\omega \eta l R^2}{\pi kT} \equiv \alpha, \tag{41}$$

where α is a dimensionless parameter characterizing magnitude of frictional forces. For example, in the case of RNA rotation during transcription in aqueous solution, substituting $\omega \approx 100$ nt/s ≈ 60 rad/s (reviewed in [29]), $\eta \approx 10^{-3}$ Pa s, $R \approx l \approx 10^{-9}$ m, $kT \approx 4 \times 10^{-21}$ J, we obtain $\alpha \approx 10^{-8}$.

We will analyze Eq. (41) for $\alpha \ll 1$, and assuming that the total length of the chain $N > 1/\alpha$. In general case, the integral of Eq. (41) over χ cannot be expressed through a finite number of elementary functions. However, for $\chi \gg 1$, we can make a substitution:

$$\chi \equiv \frac{\xi}{\ln \xi}, \tag{42}$$

and, if $\chi \gg 1$, then $\xi \gg 1$; thus

$$\ln \chi = \ln \xi - \ln (\ln \xi) \approx \ln \xi \tag{43}$$

and

$$\frac{d\chi}{ds} = \frac{d\xi}{ds} \left[\frac{1}{\ln \xi} - \left(\frac{1}{\ln \xi} \right)^2 \right] \approx \frac{d\xi}{ds} \frac{1}{\ln \xi}. \tag{44}$$

Substituting approximations Eqs. (43) and (44) into Eq. (41), we obtain

$$-\frac{1}{\xi^3} \frac{d\xi}{ds} \approx \alpha; \tag{45}$$

thus

$$\xi \sim \frac{1}{(\alpha s)^{1/2}}, \tag{46}$$

and from that, we obtain profiles along the chain length for the blob size (which in this regime is equivalent to the characteristic distance from the chain to the cylinder),

$$r_b \equiv R\chi \sim \frac{R}{(\alpha s)^{1/2}\ln(1/\alpha s)}, \tag{47}$$

and for the torque,

$$\frac{M}{kT} \sim \frac{1}{\ln\chi} \sim \frac{1}{\ln(1/\alpha s) - 2\ln[\ln(1/\alpha s)]}. \tag{48}$$

The requirement for the validity of these equations is a large normalized blob size χ, which is satisfied, as long as the distance from the free end s is sufficiently smaller than $1/\alpha$. When the distance from the free end exceeds this value, the chain becomes tightly wound around a cylinder and its radius of gyration approaches the radius of the cylinder (i.e., it would be practically independent upon torque). Consequently, viscous resistance per one segment would be also independent upon torque, and thus, further accumulation of torque would grow linearly with s.

The parameter of particular interest is the number of segments in the first blob N_{b1}, which is the characteristic number of segments starting from which nonrandom winding of the chain around the cylinder becomes pronounced. For an ideal Gaussian chain in the absence of hydrodynamic interactions it could be evaluated from Eq. (47), taking into account that $r_b(s = N_{b1}) \equiv r_{b1} \sim lN_{b1}^{1/2}$, from which we could obtain that, up to the logarithmic multiplier, $N_{b1} \sim (1/\alpha)^{1/2}$.

However, it is more convenient to evaluate N_{b1} directly from Eq. (35) for the first blob. Estimations performed for the first blob based on Eq. (35) are also applicable in the case of hydrodynamic interactions between the segments, as well as for non-ideal chains with excluded volume. In contrast, analysis for the "higher order blobs" based on Eq. (34) is applicable only in the absence of interactions between the segments, because in the case of "pure" rotation torsional blobs formed by rotating chain would be localized within each other like "Russian dolls"; thus neglecting interactions between segments within different blobs [as it was done upon derivation of Eq. (34)] is not justified. In this aspect, torsional blobs differ from tensile blobs, which are separated in space, and interactions between the segments belonging to different blobs could be neglected [39]. Of course, in the case of transcription, the rotational movement is accompanied by linear translocation along the the DNA axis; thus torsional blobs in principle become shifted relative to each other in this direction [as in the very exaggerated form shown in Fig. 1(b)] due to viscous resistance to linear translocation. However, because viscous resistance against linear translocation is expected to be much smaller than that against rotation (see below), in reality this shift would be small in comparison with the size of the blobs.

Below we will obtain the expression for the number of segments in the first blob in general form, which includes excluded volume effects and hydrodynamic interactions.

In the case of strong hydrodynamic interactions between segments (nondraining coil), Eq. (38) is replaced by

$$\mu \sim \eta\langle r^2\rangle r_b. \tag{49}$$

Combining Eqs. (38) and (49) for the large blob approximation $\langle r^2\rangle \sim r_b^2$ (one can check that the small blob approximation, in which $\langle r^2\rangle \approx R^2$, is not compatible with condition $\alpha \ll 1$) with Eqs. (26) and (30), we obtain

$$N_{b1}^{\theta}(\ln N_{b1})^{\kappa} \sim \frac{kT}{\omega\eta l^3} \sim \frac{1}{\alpha}. \tag{50}$$

where $\theta = 1 + 2\nu$ or $\theta = 3\nu$, for draining and nondraining coils, respectively; $\nu = 1/2$ and $\nu = 3/5$ for Gaussian chains and for chains with excluded volumes, respectively; $\kappa = 1$ and $\kappa = 0.5$ (or 0.75) for ideal Gaussian chains, and for chains with excluded volume, respectively [see references after Eq. (29)]. [Parameter α in Eq. (50) is assumed to be the same as in Eq. (41), because we neglect the coefficients of the order of unity, and consider the case in which $l \approx R$].

At $\alpha \ll 1$, Eq. (50) could be approximately resolved relative to N_{b1} by making a substitution,

$$N_{b1} = (1/\alpha)^{1/\theta} f(\alpha), \tag{51}$$

which upon substituting into Eq. (50) gives

$$[f(\alpha)]^{\theta}[\ln(1/\alpha)^{1/\theta} + \ln f(\alpha)]^{\kappa} = 1. \tag{52}$$

Assuming that $|\ln(1/\alpha)^{1/\theta}| > |\ln f(\alpha)|$, from Eq. (52) we obtain the result which is consistent with this assumption:

$$f(\alpha) \approx \frac{\theta^{\kappa/\theta}}{[\ln(1/\alpha)]^{\kappa/\theta}}, \tag{53}$$

and, thus from Eqs. (51) and (53) we obtain the approximate solution of Eq. (50) at $\alpha \ll 1$:

$$N_{b1} \sim \theta^{\kappa/\theta}\frac{(1/\alpha)^{1/\theta}}{[\ln(1/\alpha)]^{\kappa/\theta}}. \tag{54}$$

From Eq. (54), for $\alpha \approx 10^{-8}$ [which is relevant for transcription conditions; see estimate following Eq. (41)], the smallest value of N_{b1} which corresponds to draining coils with excluded volume ($\theta = 11/5$; $\kappa = 0.75$) is about 2×10^3; the largest, which corresponds to nondraining coils without excluded volume ($\theta = 3/2$; $\kappa = 1$), is about 4×10^4. In the case of the single-stranded RNA, for which one segment comprises about three nucleotides [40], these values would correspond to about 10^4 and about 10^5 nucleotides, respectively.

In terms of transcriptions, the above predicts that in the media with waterlike viscosity and in the absence of bound proteins, transcripts with lengths up to about 10^4 nt would rotate as unperturbed coils, and only for longer transcripts nonrandom winding around DNA becomes pronounced.

From Eq. (30), rotation of the first blob would produce torque:

$$M \sim kT/(\ln N_{b1})^{\kappa}. \tag{55}$$

The torque $M = kT$ corresponds to superhelical density 0.03 (see Appendix B). Experiments have shown that superhelical density of this magnitude could appear in *in vitro* transcription without either RNA or DNA tethering to proteins

or other bulky objects when the nascent transcript reaches the length of about 10^4 nt [41]. For that to occur, both nascent RNA and DNA must have sufficient viscous resistance to create such a torque upon their relative rotation during transcription; otherwise, if either one of them has a much lesser resistance, it would predominantly rotate (while another remains predominantly immobile), thus creating much less torque. It was shown theoretically that DNA of the lengths of about the ones which were used in these experiments could provide sufficient viscous resistance due to sequence-specific bends in DNA [29]. In terms of RNA, according to Eq. (55), the transcript about 10^4 nt (which is close to the first blob size), should create a torque which is smaller than kT by a factor roughly between 1 and 10. Thus, since in the system used by [41] several RNA polymerases were likely to transcribe one DNA template simultaneously, our estimations are consistent with creation of the total torque of about kT in this system.

Finally, in this section, we would like to analyze two "complications" of the nascent RNA dynamics during transcription in comparison with pure rotation around DNA:

First, during transcription, RNA polymerase, and consequently nascent RNA, not only rotate around, but also translocate along the DNA axis. For RNA polymerase, the ratio of the linear speed of rotation to the speed of translocation along the DNA axis is $2\pi R/H$, where $R \approx 1$ nm is the DNA radius and $H \approx 3$ nm is the DNA helical pitch. Substituting these numerical values, we obtain that for RNA polymerase, the linear speed of rotation is about twice as large as the speed of translocation. For the nascent RNA, this ratio is even larger, because its distance from the DNA axis is larger than the DNA radius. Because viscous forces are defined by the linear speed of the chain, its stretching due to translocation along the DNA axis would be smaller than due to rotation, especially for loose wrapping, where the characteristic distance between the chain segments and the cylinder axis is significantly larger than the radius of the cylinder. Thus, neglecting additional chain deformation due to translocation along the DNA axis would not significantly affect the results.

Second, the nascent RNA chain is growing during transcription. In general, this would make the rate of rotation around the DNA duplex to be somewhat smaller for the nascent RNA coil than for the RNA polymerase. For example, in the limiting case of infinitely strong viscous resistance against nascent RNA rotation, the nascent RNA would simply wrap around DNA as soon as it synthesized, and would not rotate at all.

In Appendix C, we obtain the relationship between the rate of rotation of the nascent RNA coil, ω_{coil}, and that of RNA polymerase ω:

$$\omega_{\text{coil}} = \omega\left(1 - \frac{\gamma_{\text{DNA}}}{2\pi\lambda}\bar{u}\right) = \omega\left(1 - \frac{\bar{u}}{u_{\max}}\right), \qquad (56)$$

where $\gamma_{\text{DNA}} \approx 10.5$ is the number of DNA base pairs for one helical turn in a Watson-Crick double helix, $\lambda \approx 3$ is the number of nucleotides in the Kuhn segment for the single-stranded RNA, $\bar{u}$ is the winding per RNA segment averaged over the whole RNA chain, and $u_{\max} \approx 2$ rad is the maximal possible winding per segment, at which the winding angle per one newly incorporated ribonucleotide is the same as the angle at which RNA polymerase rotates during this ribonucleotide incorporation (though technically for the Gaussian model any value of u is possible, for the RNA winding around DNA during transcription, the values of $u > u_{\max}$ do not have physical meaning; moreover, this maximal value of RNA winding corresponds to RNA stretched practically up to its geometrical limit—thus a freely jointed chain model instead of a Gaussian model should be applied, and besides, twisting deformations of the DNA duplex should be taken into account [3]). When $u < u_{\max}$, $\omega_{\text{coil}} \approx \omega$ (i.e., the effect of the chain growing upon the rate of the coil rotation is negligible for loosely wrapped coils). The case $u = u_{\max}$ corresponds to infinitely large viscous resistance of the coil, when the coil stops rotating, which is equivalent to the RNA anchoring without initial slack. In reality, RNA invasion into the DNA duplex is likely to occur before this value is reached (see below).

D. Possible experimental testing and potential biological significance of the theoretical results

Testing torque-winding interdependence. Although we primarily discuss RNA winding around DNA in the context of cotranscriptional RNA anchoring or viscous impediment, the torque-winding interdependence for the RNA wound around DNA, in principle, could be tested in a simplified system without transcription.

One possibility would be to use single-molecule manipulations, which permit application of a torque and a stretching force to a single molecule (or to a single defined complex of several molecules; reviewed in [42–44]). One of the possible experimental designs, shown in Fig. 2, is a "braiding" system, which was originally applied to study topoisomerase action upon intertwined DNA duplexes [45–47]. In this assay, two molecules (in our case, single-stranded RNA and double-stranded DNA) could be attached (in parallel fashion) by one end to an immobile surface, and by the other end to a bead which could be rotated (e.g., using magnetic tweezers [45]), thus causing intertwining of the molecules and creating a torque acting upon the bead. In the magnetic tweezers-based experiments it is possible to track the winding angle and the torque [48]; thus, the experimental torque-winding dependence could be obtained and compared with our theoretical results. Note that in the braiding assay, a single-strand break could be introduced into the DNA duplex [45,46]; this would act like a swivel, preventing accumulation of the twisting deformation within the duplex upon the bead rotation. Thus, the torque created in this system would be solely due to RNA winding around DNA.

Because the mechanical properties of single-stranded RNA and single-stranded DNA are similar, single-stranded RNA could be replaced by single-stranded DNA in these experiments, in case that would simplify experimental procedures. Also, to facilitate an attachment of ssRNA (or ssDNA) and dsDNA to the same bead and to render their points of attachment sufficiently close to each other, they could be designed to form a local acidic pH-dependent triplex (reviewed in [25]). That could hold them together prior to the attachment to the bead and to the surface, and then the triplex could be dissociated after their attachment by increasing the pH.

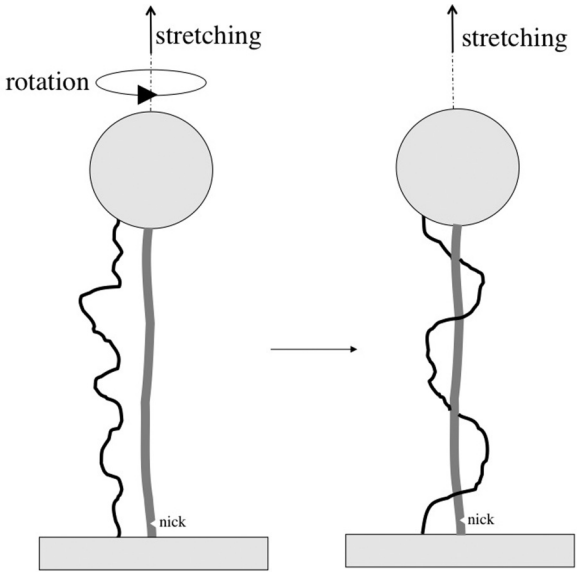

FIG. 2. Possible testing of torque-winding interdependence in single-molecule experiments. Single-stranded (ss)RNA and double-stranded (ds) DNA are show as a thinner black and a thicker gray line, respectively. A (magnetic) bead and immobile surface are shown as a light gray circle and light gray rectangle, respectively. A torque applied to the bead allows the rotation of it, thus intertwining RNA and DNA. A stretching force applied to the bead allows keeping DNA in sufficiently straight configuration, while the single-stranded RNA, whose contour length is about twice as large, would remain loose. A nick in dsDNA acts like a swivel, preventing accumulations of torque within the DNA duplex upon the bead rotation; thus a torque created in the system would be solely due to RNA-DNA intertwining.

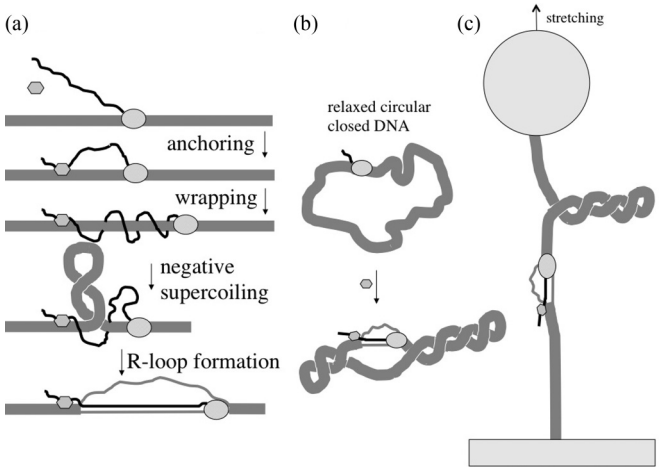

FIG. 3. Predicted effects of cotranscriptional nascent RNA anchoring and their possible experimental detection. Designations are the same as in Fig. 1. (a) Anchoring-induced RNA winding around DNA would first generate negative supercoiling within RNA-wound region. If this region is longer than the DNA persistent length, and the DNA is not strongly stretched by some external forces, this supercoiling could lead to formation of a DNA plectoneme(s) in the wrapped region, as shown; otherwise supercoiling would be only in the form of DNA twisting. Further increase in RNA winding density, and consequently in negative supercoiling, would lead to the RNA invasion in DNA, i.e., *R*-loop formation. (b), (c) Within circular closed relaxed DNA (b) this negative supercoiling and/or *R*-loop formation (only the latter is shown) would create compensatory positive supercoiling outside the DNA region between the anchoring point and RNA polymerase. In the single-molecule experiment (c), where non-nicked linear DNA is attached by one end to some immobile surface, and the by the other end is attached to a magnetic bead, this supercoiling and/or *R*-loop formation (only the latter is shown) could either create plectonemic superturns, or could be completely in the twisting form, depending upon an external stretching force applied to the DNA.

Potential biological role and experimental testing of the predicted effects of cotranscriptional nascent RNA anchoring to DNA. As already mentioned in the Introduction (see also review [49]), it is plausible that cotranscriptional nascent RNA anchoring to DNA could occur *in vivo* either by proteins which could bind RNA and DNA simultaneously, or by direct RNA-DNA interactions.

According to our model [Fig. 3(a)], this anchoring would cause nascent RNA winding around DNA, creating a torque acting upon the DNA duplex. This torque induces negative superhelical stress in the DNA duplex region between the anchoring point and transcribing RNA polymerase (i.e., within the RNA-wound DNA region) (see Appendix B). If the RNA-wound DNA region is longer than the DNA persistent length, and the DNA is not strongly stretched by some external forces, this supercoiling could lead to the formation of a DNA plectoneme in this region [Fig. 3(a), the second scheme from the bottom]; otherwise, supercoiling would be seen only in the form of DNA twisting.

After the anchoring has occurred, the RNA winding around DNA becomes tighter upon continuation of transcription and eventually, if nothing else happens, this would attain a limiting value of very tight winding density, which corresponds to the situation in which RNA is anchored to DNA at the very beginning of transcription without initial slack. However, our previous estimates [3] have shown that the negative superhelical strain created by that tight RNA winding is sufficient to cause DNA duplex unwinding; thus, it seems most likely that the nascent RNA would invade the DNA duplex (thus "canceling" RNA winding around the duplex and relaxing negative superhelical stress) [Fig. 3(a), the very bottom scheme] before the winding density reaches this limiting value.

RNA invasion into DNA (i.e., *R*-loop formation) is implicated in numerous biological processes, both regulatory [6–9] and deleterious [10,11], and it is tempting to speculate that anchoring-induced *R*-loop formation (that could be modulated, for example, by concentration of the anchoring agent) might have regulatory functions in living cells.

There are a number of methods to detect *R* loops, for example, by specific chemical and enzymatic reactivity of a displaced DNA strand, or by retention of (radioactively) labeled RNA within DNA (reviewed in [50]), that could be used to test our hypothesis that cotranscriptional nascent RNA anchoring would eventually lead to *R*-loop formation.

Anchoring-induced negative supercoiling could also facilitate unusual DNA structure (e.g., cruciforms, Z- or H-DNA, reviewed in [51]) formation in the nascent RNA-wound region of DNA, provided that this area contained appropriate DNA sequences. For example, an interesting situation could

appear in the case of the Z-DNA binding protein, which is also an RNA-editing enzyme (reviewed in [21,22]). It was hypothesized that this protein, while bound to Z-DNA in the vicinity of the transcription site, could cotranscriptionally modify the nascent RNA [21,22]. It is likely that this RNA modification is associated with transient RNA binding (i.e., RNA anchoring). If there are more Z-DNA forming sequences localized between the anchoring point and transcribing RNA polymerase, then RNA-anchoring-induced negative supercoiling would facilitate B-to-Z transitions within these sequences, thus recruiting more Z-DNA binding proteins, i.e., in effect mediating "cooperativity" of protein binding.

If cotranscriptional RNA anchoring followed by generation of negative supercoiling and/or *R*-loop formation within the RNA-wound region occurred within relaxed circular closed DNA, a compensatory positive supercoiling would appear in the DNA outside the RNA-wound (or *R*-loop-forming) region [Fig. 3(b)]. This supercoiling could be detected, for example, by first treating the plasmid with topoisomerase IV, to preferentially relax positive supercoils [46], and then removing RNA by RNase treatment. The entire procedure would convert the plasmid from relaxed form to negatively supercoiled, which could be detected by altered plasmid mobility in gel.

Alternatively, compensatory positive supercoiling could be detected in single-molecule experiments [Fig. 3(c)], for example, by monitoring either torque-induced rotation of the bead, or by monitoring vertical shift of the bead position due to DNA buckling caused by formation of plectonemic supercoils (e.g., in assay similar to the one used in [52]).

Similar effects are expected in the case of dynamic transcription-induced supercoiling (e.g., [41]); however, in contrast to transcription dynamic supercoiling, RNA-anchoring-induced supercoiling would not require a long transcript to create sufficient viscous resistance and, importantly, it would persist even when polymerase is paused or stalled, provided that the transcription complex is not dissociated from the template. (Note that if an *R* loop is formed, for certain sequences it would persist after dissociation of the transcription complex even in positively superhelical DNA, due to the superior stability of RNA-DNA versus DNA-DNA duplexes for these sequences).

Both RNA-winding-induced strain [3] and *R*-loop formation [3,12–14] are expected to interfere with transcription, and might lead to transcription slowing down, pausing, or stalling. These effects could be also monitored in single-molecule experiments (e.g., [53,54]).

In the experiments described above, a model artificial anchoring agent could be used: For example, it could be a bivalent oligonucleotide that is comprised of two moieties, one of which forms a triplex with double-stranded DNA, and the other forms a duplex with the single-stranded nascent RNA. These kinds of artificial anchoring agents, in principle, could be used to target *R*-loop formation to specific sequences, which potentially could be used for artificial gene regulation.

III. CONCLUSIONS

(1) We analyzed the behavior of a long Gaussian chain wound around a cylinder by a constant torque, and have obtained interdependences between torque, free energy of the chain, an average winding per one chain segment, and an intrinsic characteristic spatial scale of the chain (the torsional blob size). All these dependences are expressed via the function $x_1(q)$, where x_1 is the largest zero of the modified Bessel function of purely imaginary order iq, and q is the torque normalized upon thermal energy kT. Though the general analytical expression for the function $x_1(q)$ is unknown, a numerical solution and analytical asymptotics are available. Using the simplified blob-based approach, we extended our analysis to nonideal polymer chains. The obtained torque-winding dependence can be used to estimate strains which appear in DNA and RNA during transcription, when nascent RNA becomes anchored to DNA, for example, via bivalent protein binding.

(2) Using the interdependence between characteristic spatial scale (the blob size) of the chain and the torque, we extended our analysis to a polymer chain with one free end, rotating in viscous solution. In particular, we estimated the minimal length of the chain, starting from which nonrandom winding of the chain around the cylinder became pronounced. For RNA during transcription, this length estimate is around 10^4 nucleotides. Thus, in the absence of anchoring or some protein binding that increases viscous resistance, the winding around DNA is pronounced only for sufficiently long transcripts.

(3) We estimated a correction introduced when the RNA chain is growing during its rotation around DNA. We concluded that this correction is not important for loosely wound RNA, but that it becomes increasingly important with increasing of RNA winding.

(4) We suggested several experimental approaches to test theoretical predictions of our analysis.

ACKOWLEDGMENTS

I thank Professor P. C. Hanawalt, in whose laboratory this work was performed, for support, critical reading of the manuscript, and helpful suggestions, and Professor A. Y. Grosberg for helpful discussions and suggestions. The work was supported by Grant No. CA077712 from the National Cancer Institute, NIH, to the Hanawalt Laboratory at Stanford University.

APPENDIX A: CHARACTERISTIC DISTANCE FROM THE CHAIN TO THE SURFACE OF THE CYLINDER AT LARGE TORQUES

We are going to analyze behavior of the chain in the vicinity of the cylinder surface at large torques. For this purpose, we first rewrite Eq. (10) in the form

$$\frac{d^2g}{d\,(\ln x)^2} + (q^2 - x^2)g = 0. \tag{A1}$$

For a point at position x, the distance from the surface is

$$y = x - x_1. \tag{A2}$$

In the close vicinity of the surface, i.e., when $y \ll x_1$,

$$\ln x = \ln(x_1 + y) = \ln x_1 + \ln\left(1 + \frac{y}{x_1}\right) \approx \ln x_1 + \frac{y}{x_1} \tag{A3}$$

and

$$q^2 - x^2 = (q-x)(q+x) = (q - x_1 - y)(q + x_1 + y) \approx (q - x_1 - y)(q + x_1). \quad \text{(A4)}$$

Note that because we are interested in $y \ll x_1$ we omitted y in the term $(q + x_1 + y)$, but not in the term $(q - x_1 - y)$, because at large torques (i.e., large q) $q - x_1 \ll x_1$ [30].

Substituting Eqs. (A3) and (A4) into Eq. (A1), we obtain

$$x_1^2 \frac{d^2 g}{dy^2} + (q - x_1 - y)(q + x_1)\, g = 0. \quad \text{(A5)}$$

This equation can be simplified by linear substitution,

$$y = \left(\frac{x_1^2}{q + x_1}\right)^{1/3} t + (q - x_1), \quad \text{(A6)}$$

which converts it into an Airy equation, which, in contrast to a Bessel equation, does not contain any parameters:

$$\frac{d^2 g}{dt^2} - tg = 0. \quad \text{(A7)}$$

We are interested in a solution which approaches zero when $t \to \infty$. This solution is the Airy function of the first kind $\mathrm{Ai}(t)$. From $t = -\infty$ up to a certain negative value $t = t_1$ (further referred to as the largest zero of the function), this function is oscillating between negative and positive values until it switches from negative to positive value for the last time at $t = t_1$, and then remains positive, first reaching a local maximum, and then monotonically decreasing, approximately as $\exp(-\frac{2}{3}t^{3/2})/t^{1/4}$.

The maximal zero of this function $t_1 = -2.3381\ldots$ must correspond to the surface of the cylinder, i.e., $y = 0$. Thus, from Eq. (A6),

$$q - x_1 = -\left(\frac{x_1^2}{q + x_1}\right)^{1/3} t_1 \approx 2\left(\frac{x_1^2}{q + x_1}\right)^{1/3} \approx 2^{2/3} x_1^{1/3} \approx 2^{2/3} q^{1/3} \approx 1.6\, q^{1/3} \quad \text{(A8)}$$

(here we took into account that $q - x_1 \ll x_1$ provided that q is large, thus $q + x_1 \approx 2q \approx 2x_1$). This result is similar to the estimate obtained in [30]:

$$q = x_1 + \frac{1}{2}\left(\frac{9\pi}{4}\right)^{2/3} x_1^{1/3} + \cdots \approx x_1 + 1.8 x_1^{1/3} \quad \text{(A9)}$$

(Eq. (18) in [30]; designations are modified in accordance with the current paper).

Because Eq. (A7) does not contain any parameters, and, taking into account Eq. (A8), the coefficients in Eq. (A6) both scale as $q^{1/3}$; the characteristic scale for y is

$$y_c = q^{1/3}. \quad \text{(A10)}$$

Thus, the characteristic distance from the surface at large torques is

$$h_c \sim y_c \frac{R}{x_1} \approx q^{1/3}\frac{R}{x_1} \approx q^{1/3}\frac{R}{q} = \frac{R}{q^{2/3}} \equiv \frac{R}{\left(\frac{M}{kT}\right)^{2/3}} \sim \frac{l^{4/3}}{u^{2/3} R^{1/3}}. \quad \text{(A11)}$$

The second part of this equation is obtained by substitution of Eq. (23).

APPENDIX B: SUPERCOILING INDUCED BY COTRANSCRIPTIONAL NASCENT RNA ANCHORING TO DNA

As already stated, anchoring of the nascent RNA to DNA during transcription causes the nascent RNA winding around DNA, which exerts torque upon DNA. This torque causes deformation within DNA (superhelical strain), and these deformations, in turn, decrease RNA winding around DNA. Below, we will obtain a connection between degree of RNA winding and superhelical strain within DNA in general form. We will model RNA as a flexible chain, and DNA as an elastic cylinder.

First consider the situation in which the cylinder is straight and its deformation under the torque could be neglected (i.e., either the cylinder is very rigid, or the torque is sufficiently small). In this case, the average winding angle per one segment of wrapped RNA is

$$u = \frac{\frac{2\pi}{\gamma_{\mathrm{DNA}}}(\mathrm{N_{RNA}} - \mathrm{N_{RNA,0}})}{\frac{\mathrm{N_{RNA}}}{\lambda_{\mathrm{RNA}}}}, \quad \text{(B1)}$$

where $\mathrm{N_{RNA}}$ and $\mathrm{N_{RNA,0}}$ is the nascent RNA length (in nucleotides) between RNA polymerase and the anchoring point at the current moment and at the moment of anchoring, respectively; $\lambda_{\mathrm{RNA}} \approx 3$ [40] is the number of RNA nucleotides in an apparent segment, and $\gamma_{\mathrm{DNA}} \approx 10.5$ is number of DNA bases for one DNA helical turn (which is the same as the number of RNA nucleotides synthesized during one turn of RNA polymerase around DNA).

In the next approximation, the cylinder is still straight, but it is capable of twisting deformations under the torque, which partially relax the torque. In terms of DNA, that approximation could be valid, either for sufficiently short DNA fragment (<300 bp), or if the DNA is stretched by some external force. In this case, if the twisting angle of the cylinder is φ (note that φ has an opposite sign relative to that of the winding angle $\phi \equiv Nu$, and because ϕ is positive, φ is negative) Eq. (B1) is transformed into

$$u = \frac{\frac{2\pi}{\gamma_{\mathrm{DNA}}}(\mathrm{N_{RNA}} - \mathrm{N_{RNA,0}}) + \varphi}{\frac{\mathrm{N_{RNA}}}{\lambda_{\mathrm{RNA}}}} = \frac{\frac{2\pi}{\gamma_{\mathrm{DNA}}}(\mathrm{N_{RNA}} + \mathrm{N_{DNA}}\sigma - \mathrm{N_{RNA,0}})}{\frac{\mathrm{N_{RNA}}}{\lambda_{\mathrm{RNA}}}}, \quad \text{(B2)}$$

where

$$\sigma = \frac{\frac{\varphi}{2\pi}}{\frac{\mathrm{N_{DNA}}}{\gamma_{\mathrm{DNA}}}} \quad \text{(B3)}$$

is superhelical density, and $\mathrm{N_{DNA}}$ is the number of DNA base pairs between the anchoring point and the transcribing RNA polymerase. (If the anchoring occurs at the unique DNA sequence homologous to the bound region of RNA, then $\mathrm{N_{DNA}} = \mathrm{N_{RNA}}$).

The energy of supercoiling within wrapped DNA region is

$$G_{sc} = \mathrm{N_{DNA}} A \sigma^2, \quad \text{(B4)}$$

where A is a coefficient of elasticity. The supercoiling creates "countertorque,"

$$M_\sigma(\sigma) = \frac{\partial G_{sc}}{\partial \varphi} = 2A\mathrm{N}_{\mathrm{DNA}}\sigma\frac{\partial \sigma}{\partial \varphi} = A\frac{\gamma_{\mathrm{DNA}}}{\pi}\sigma, \tag{B5}$$

which equilibrates torque from the strain in the wrapped chain:

$$M_\sigma(\sigma) = -M(u). \tag{B6}$$

Thus

$$\sigma = -\frac{\pi}{\gamma_{\mathrm{DNA}}A}M(u), \tag{B7}$$

and Eq. (B2) becomes

$$u = \frac{\frac{2\pi}{\gamma_{\mathrm{DNA}}}\left[\mathrm{N}_{\mathrm{RNA}} - \mathrm{N}_{\mathrm{DNA}}\frac{\pi}{\gamma_{\mathrm{DNA}}A}M(u) - \mathrm{N}_{\mathrm{RNA},0}\right]}{\frac{\mathrm{N}_{\mathrm{RNA}}}{\lambda_{\mathrm{RNA}}}}. \tag{B8}$$

By substituting the dependence $M(u)$ [or $u(M)$] [obtained for a given polymer model of RNA, e.g., Eqs. (18) or (23) for an ideal Gaussian chain] into Eq. (B8) and resolving it relative to u (or M) one can estimate both the torque and an average winding angle for given lengths of the transcripts $\mathrm{N}_{\mathrm{RNA}}$ and $\mathrm{N}_{\mathrm{RNA},0}$, and then from Eq. (B7) estimate superhelical density.

Long, nonstretched supercoiled DNA adopts a three-dimensional structure mostly comprised of plectonemic supercoils ([55–58] and references therein); thus, it cannot be modeled by a straight cylinder. However, we think that in this case the behavior of wrapped RNA also could be roughly described as "two dimensional:" At sufficiently loose winding, the DNA plectonemes would tend to extrude from the wrapped area, and most of the wrapping would occur around relatively straight DNA linkers between plectonemic regions. In contrast, for the tight winding, RNA would be close to the DNA surface, thus relatively insensitive to the overall shape of DNA contour. Thus, in both cases wrapping around a straight cylinder might still be a reasonable approximation.

For the long, nonstretched DNA, parameter A in Eq. (B7) is

$$A = 10kT \tag{B9}$$

(reviewed in [55,56]), and the superhelical density [Eq. (50)] becomes

$$\sigma = -\frac{\pi}{10\gamma}\frac{M}{kT} \approx -0.03\frac{M}{kT} \equiv -0.03q. \tag{B10}$$

Most biologically interesting values of σ are roughly in the interval from -0.03 to -0.1, which corresponds to superhelical densities in various circular DNAs isolated from various organisms (reviewed in [59]) and are likely to reflect the actual level of supercoiling which might occur *in vivo*. In this region of σ, double-stranded Watson-Crick B form of DNA with random sequence is stable at physiological conditions, but supercoiling-induced melting and other supercoiling-induced structural transitions such as cruciform, Z-, and H-DNA formation could occur locally at some specific sequences (reviewed in [56]). This interval of σ values corresponds to q between 1 and 3 (i.e., about unity), which is in the transitional area, where simple analytical approximations for function $x_1(q)$, and, consequently for torque-winding dependence [Eq. (13)] are not available. However, in this area torque-winding dependence could be obtained numerically, e.g., using numerical evaluation of function $x_1(q)$ [30].

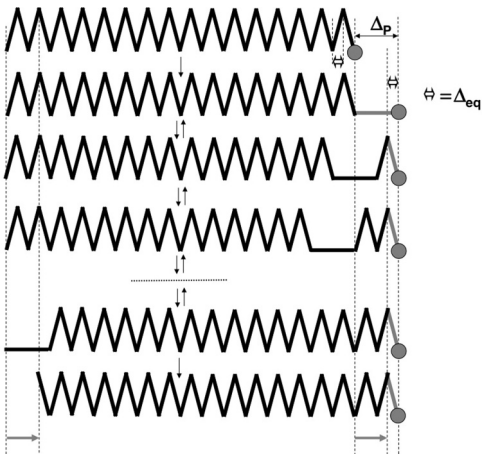

FIG. 4. Schematic representation for simultaneous movement and growing of the nascent RNA. For explanation, see text.

APPENDIX C: CHAIN ROTATION ACCOMPANIED BY GROWING

To make derivation easier, we will schematically visualize rotational movement of polymerase and the nascent RNA chain as linear translocation (Fig. 4), and at the end, replace linear translocational shifts by angular rotational shifts.

Consider a "snapshot" of RNA polymerase (symbolized by the gray circle), to which a coil of the nascent RNA (shown in black) is attached (Fig. 4, top). The chain is considered to be in the "equilibrium" stretched state (diagrammatically shown by a zigzag pattern formed by the chain segments), in which the average projection of the chain segment upon the direction of polymerase movement is Δ_{eq}. Next, during an interval of time Δt_P, polymerase synthesizes a new segment (shown in gray) and simultaneously moves the distance Δ_P (i.e., the velocity of polymerase is $\upsilon_P = \Delta_P/\Delta t_P$). The newly synthesized segment, which is initially overstretched in comparison with the rest of the coil, is "equilibrated" into the coil, so its projection upon direction of movement, which initially was Δ_P, becomes Δ_{eq}, as for the rest of the segments.

If the time of the segment equilibration into the coil is sufficiently smaller than the time of the segment synthesis Δt_P, we can neglect the equilibration time and assume that the whole coils shifts at the distance $\Delta_P - \Delta_{eq}$ (shown by the gray arrow) during the time Δt_P; thus, the velocity of the coil is

$$\upsilon_{\mathrm{coil}} = \frac{\Delta_P - \Delta_{eq}}{\Delta t_P} = \upsilon_P\left(1 - \frac{\Delta_{eq}}{\Delta_P}\right). \tag{C1}$$

The assumption that the segment equilibration time could be smaller than the time of the segment synthesis seems to be reasonable, or at least not contradictory, for the chains with the number of segments about or less than 10^4: If we assume that the distortion propagation along the chain occurs via a random-walk-like process, with an elementary step corresponding to local "isomerization" in which two neighboring segments "exchange" stretched and relaxed states

with each other without affecting other segments (Fig. 4), then this elementary step would involve rotational diffusion movement of roughly one segment upon roughly one turn, for which the characteristic time would be

$$\tau_0 \sim \frac{\eta l^3}{kT}, \tag{C2}$$

and the total time of equilibration,

$$\Delta t_{eq} = N^2 \tau_0, \tag{C3}$$

and

$$\frac{\Delta t_{eq}}{\Delta t_P} = N^2 \frac{\tau_0}{\Delta t_P} \approx N^2 \frac{\eta l^3}{\Delta t_P kT}. \tag{C4}$$

The fast equilibrating coil approximation is applicable when this ratio is less than unity, i.e., when

$$N < N_{eq} = \sqrt{\frac{\Delta t_P kT}{\eta l^3}}. \tag{C5}$$

Substituting numerical values $\Delta t_P \approx 3 \times 10^{-2}$ s, $\eta \approx 10^{-3}$ Pa s, $l \approx 10^{-9}$ m, $kT \approx 4 \times 10^{-21}$ J, we obtain N_{eq} about 10^4 segments.

To modify Eq. (C1) for rotational movement, Δ_{eq} should be replaced by $\bar{u}$, which is the winding per RNA segment averaged over the whole RNA chain, and Δ_P should be replaced by the angle upon which RNA polymerase has rotated around DNA while synthesizing one RNA segment,

$$\Delta_P = 2\pi\lambda/\gamma_{\mathrm{DNA}}, \tag{C6}$$

where $\gamma_{\mathrm{DNA}} \approx 10.5$ is the number of DNA base pairs for one helical turn in a Watson-Crick double helix, and $\lambda \approx 3$ is the number of nucleotides in the Kuhn segment for the single-stranded RNA.

Substituting these expressions for Δ_{eq} and Δ_P in Eq. (C1), and replacing linear translocation rate υ by rotational rate ω, we obtain Eq. (56) of the main text.

In general, the chain-averaged winding per segment $\bar{u}$ could be obtained from torque profiles (see Sec. II C) using torque-winding interdependence. However, here we will consider only a simple special case of "viscous anchoring" (Fig. 5), in which

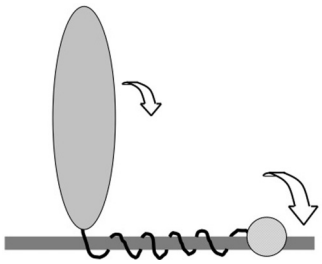

FIG. 5. Viscous RNA anchoring. RNA polymerase is shown as a smaller gray oval, and a bulky object attached to the end of RNA is shown as a larger gray oval. It rotates more slowly than RNA polymerase, which is symbolized by a smaller block arrow.

the end of the nascent RNA is attached to some bulky object [for example, large protein(s)], and the viscous resistance of this object, μ, is much larger than the viscous resistance of the RNA; thus the latter could be neglected. In this case the torque would be the same for all regions of the chain and equivalent to

$$M = \mu\omega_{\mathrm{coil}}. \tag{C7}$$

Here we took into account that in the steady state the RNA coil and the bulky object attached to the end are rotating with the same speed.

Consequently, the average winding per segment would be the same for all regions of the coil, and in the case of sufficiently tight winding [Eq. (23)],

$$\bar{u} \approx \left(\frac{l}{R}\right)^2 \frac{M}{kT} = \left(\frac{l}{R}\right)^2 \frac{\omega_{\mathrm{coil}}\mu}{kT}. \tag{C8}$$

Substituting this in Eq. (56), we can obtain the rotational rate of the coil,

$$\omega_{\mathrm{coil}} = \frac{\omega}{1 + \frac{1}{2\pi}\frac{\gamma_{\mathrm{DNA}}}{\lambda}\left(\frac{l}{R}\right)^2 \frac{\omega\mu}{kT}}, \tag{C9}$$

and the torque,

$$M = \mu\omega_{\mathrm{coil}} = \frac{\omega\mu}{1 + \frac{1}{2\pi}\frac{\gamma_{\mathrm{DNA}}}{\lambda}\left(\frac{l}{R}\right)^2 \frac{\omega\mu}{kT}}. \tag{C10}$$

[1] S. F. Edwards, Proc. Phys. Soc. **91**, 513 (1967).
[2] A. Grosberg and H. Frisch, J. Phys. A: Math. Gen. **36**, 8955 (2003).
[3] B. P. Belotserkovskii and P. C. Hanawalt, Biophys. J. **100**, 675 (2011).
[4] A. Papantonis and P. R. Cook, Transcription **2**, 41 (2011).
[5] C. N. Tennyson, H. J. Klamut, and R. G. Worton, Nat. Genet. **9**, 184 (1995).
[6] T. A. Baker and A. Kornberg, Cell **55**, 113 (1988).
[7] H. Masukata, S. Dasgupta, and J. Tomizawa, Cell **51**, 1123 (1987).
[8] F. T. Huang, K. Yu, C. L. Hsieh, and M. R. Lieber, Proc. Natl. Acad. Sci. USA **103**, 5030 (2006).
[9] N. Maizels, Nat. Struct. Mol. Biol. **13**, 1055 (2006).
[10] Y. Lin, S. Y. Dent, J. H. Wilson, R. D. Wells, and M. Napierala, Proc. Natl. Acad. Sci. USA **107**, 692 (2010).
[11] A. Aguilera and T. Garcia-Muse, Mol. Cell **46**, 115 (2012).
[12] M. M. Krasilnikova, G. M. Samadashwily, A. S. Krasilnikov, and S. M. Mirkin, EMBO J. **17**, 5095 (1998).
[13] B. P. Belotserkovskii, R. Liu, S. Tornaletti, M. M. Krasilnikova, S. M. Mirkin, and P. C. Hanawalt, Proc. Natl. Acad. Sci. USA **107**, 12816 (2010).
[14] B. P. Belotserkovskii, A. J. Neil, S. S. Saleh, J. H. Shin, S. M. Mirkin, and P. C. Hanawalt, Nucl. Acids Res. **41**, 1817 (2013).
[15] P. C. Hanawalt, Science **266**, 1957 (1994).
[16] P. C. Hanawalt and G. Spivak, Nat. Rev. Mol. Cell Biol. **9**, 958 (2008).
[17] D. Roy and M. R. Lieber, Mol. Cell Biol. **29**, 3124 (2009).

[18] Y. Jeon and J. T. Lee, Cell **146**, 119 (2011).
[19] J. T. Lee, Science **338**, 1435 (2012).
[20] S. W. Blume, Z. Meng, K. Shrestha, R. C. Snyder, and P. D. Emanuel, J. Cell Biochem. **88**, 165 (2003).
[21] A. Herbert and A. Rich, J. Biol. Chem. **271**, 11595 (1996).
[22] A. Herbert and A. Rich, Genetica **106**, 37 (1999).
[23] K. M. Schmitz, C. Mayer, A. Postepska, and I. Grummt, Genes Dev. **24**, 2264 (2010).
[24] I. Martianov, A. Ramadass, A. Serra Barros, N. Chow, and A. Akoulitchev, Nature **445**, 666 (2007).
[25] M. D. Frank-Kamenetskii and S. M. Mirkin, Annu. Rev. Biochem. **64**, 65 (1995).
[26] S. M. Mirkin and M. D. Frank-Kamenetskii, Annu. Rev. Biophys. Biomol. Struct. **23**, 541 (1994).
[27] P. H. Wanrooij, J. P. Uhler, Y. Shi, F. Westerlund, M. Falkenberg, and C. M. Gustafsson, Nucl. Acids Res. **40**, 10334 (2012).
[28] L. F. Liu and J. C. Wang, Proc. Natl. Acad. Sci. USA **84**, 7024 (1987).
[29] P. Nelson, Proc. Natl. Acad. Sci. USA **96**, 14342 (1999).
[30] E. M. Ferreira and J. Sesma, Numer. Math. **16**, 278 (1970).
[31] A. Y. Grosberg and A. R. Khokhlov, *Statistical Physics of Macromolecules* (Springer-Verlag, New York, 1994).
[32] P. Pincus, Macromolecules **9**, 386 (1976).
[33] B. Drossel and M. Kardar, Phys. Rev. E **53**, 5861 (1996).
[34] J. Rudnick and Y. Hu, Phys Rev. Lett. **60**, 712 (1988).
[35] J.-C. Walter, G. T. Barkema, and E. Carlon, J. Stat. Mech.: Theory Exp. (2011) P10020.
[36] F. Brochard-Wyart, Europhys. Lett. **23**, 105 (1993).
[37] F. Brochard-Wyart, H. Hervet, and P. Pincus, Europhys. Lett. **26**, 511 (1994).
[38] F. Brochard-Wyart, Europhys. Lett. **30**, 387 (1995).
[39] P. Rowghanian and A. Y. Grosberg, Phys. Rev. E **86**, 011803 (2012).
[40] S. B. Smith, Y. Cui, and C. Bustamante, Science **271**, 795 (1996).
[41] Y. P. Tsao, H. Y. Wu, and L. F. Liu, Cell **56**, 111 (1989).
[42] C. Bustamante, Z. Bryant, and S. B. Smith, Nature **421**, 423 (2003).
[43] Z. Bryant, F. C. Oberstrass, and A. Basu, Curr. Opin. Struct. Biol. **22**, 304 (2012).
[44] M. H. Larson, R. Landick, and S. M. Block, Mol. Cell **41**, 249 (2011).
[45] G. Charvin, D. Bensimon, and V. Croquette, Proc. Natl. Acad. Sci. USA **100**, 9820 (2003).
[46] M. D. Stone, Z. Bryant, N. J. Crisona, S. B. Smith, A. Vologodskii, C. Bustamante, and N. R. Cozzarelli, Proc. Natl. Acad. Sci. USA **100**, 8654 (2003).
[47] G. Charvin, A. Vologodskii, D. Bensimon, and V. Croquette, Biophys. J. **88**, 4124 (2005).
[48] J. Lipfert, J. J. Kerssemakers, M. Rojer, and N. H. Dekker, Rev. Sci. Instrum. **82**, 103707 (2011).
[49] B. P. Belotserkovskii, S. M. Mirkin, and P. C. Hanawalt, Chem. Rev. **113**, 8620 (2013).
[50] K. Yu, D. Roy, F. T. Huang, and M. R. Lieber, Methods Enzymol. **409**, 316 (2006).
[51] S. M. Mirkin, Front. Biosci. **13**, 1064 (2008).
[52] M. Nollmann, M. D. Stone, Z. Bryant, J. Gore, N. J. Crisona, S. C. Hong, S. Mitelheiser, A. Maxwell, C. Bustamante, and N. R. Cozzarelli, Nat. Struct. Mol. Biol. **14**, 264 (2007).
[53] M. H. Larson, W. J. Greenleaf, R. Landick, and S. M. Block, Cell **132**, 971 (2008).
[54] J. Ma, L. Bai, and M. D. Wang, Science **340**, 1580 (2013).
[55] A. V. Vologodskii, S. D. Levene, K. V. Klenin, M. Frank-Kamenetskii, and N. R. Cozzarelli, J. Mol. Biol. **227**, 1224 (1992).
[56] A. V. Vologodskii, *Topology and Physics of Circular DNA* (CRC Press, Boca Raton, FL, 1992).
[57] J. F. Marko and E. D. Siggia, Science **265**, 506 (1994).
[58] J. F. Marko and E. D. Siggia, Phys. Rev. E **52**, 2912 (1995).
[59] W. R. Bauer, Annu. Rev. Biophys. Bioeng. **7**, 287 (1978).